Efficiency, products and mechanisms of ethyl acetate oxidative degradation in air non-thermal plasma

Renato Perillo, Elena Ferracin, Agata Giardina, Ester Marotta* and Cristina Paradisi

Department of Chemical Sciences, Università di Padova, via Marzolo 1, 35131 Padova, Italy

E-mail: ester.marotta@unipd.it

Abstract

Ethyl acetate (EA) is a popular solvent and diluent in many products and one of the most ubiquitous organic pollutants of indoor air. Although EA's ascertained toxicity is classified as low, exposure to its vapors at concentrations $\geq$ 400 ppm causes serious problems in humans. EA is thus a frequent target in testing novel technologies for air purification. We report here an investigation of EA oxidative degradation in air at room temperature and atmospheric pressure induced by corona discharges. Three corona regimes, dc-, dc+ and pulsed+, were tested in the same reactor under various experimental conditions with regard to EA initial concentration (C_0) and the presence of humidity in the system. The EA degradation process was monitored by GC-FID, GC-MS and FT-IR analysis of the treated gas. These analyses yielded the concentration of residual of EA (C) and those of its major products of oxidation (CO_2, CO) and revealed a few organic reaction intermediates formed along the oxidation chain. The process energy efficiency was determined as energy constant, k_E ($kJ^{-1} \cdot L$) and as energy yield, EY ($g \cdot kW^{-1} h^{-1}$). The efficiency depends on the type of corona (pulsed+ > dc- > dc+), on the presence of humidity in the air (improvement in the case of dc-, little or no effect for dc+) and on C_0 (k_E increases linearly with $1/C_0$,). CO_2 and CO were the major carbon containing products, confirming the strong oxidizing power of air non-thermal plasma. Acetic acid and acetaldehyde were detected in very small amounts as reaction intermediates. The experimental results obtained in this work support the conclusion that different reactive species are involved in the initial step of EA oxidation in the case of dc- and dc+ corona air non-thermal plasma.

Introduction

Non-thermal plasma (NTP) is being actively pursued as an innovative option for air purification, being quite effective in the oxidative degradation of volatile organic compounds (VOCs) [1-4]. NTPs are non-equilibrium plasmas in which electron temperatures of up to 10^5 K can be reached while the bulk gas temperature remains almost unaltered and are especially useful for treating pollutants present in low concentrations [5]. Many different approaches to the generation of NTP (electron beam, dielectric barrier discharges, corona discharges, gliding arc discharges) and reactor designs and configurations have been described in the literature and new ones continue to emerge (see for example [6]). Great impulse is also given to the search and development of synergic combinations of plasma with catalysts and photocatalysts [7-12].

For practical applications, optimization of the process efficiency is a major goal and a complex task to carry out because of the concurrence of many experimental variables. To make progress in this direction it is important to gain good insight into the interplay of all these effects. With this intent we chose ethyl acetate (EA) as model VOC, for reasons specified below, and studied the dependence of its NTP induced degradation efficiency on the following experimental variables, which were changed one at a time: the type of energization used, the ethyl acetate initial concentration, the presence of humidity in the air. Besides the energy efficiency, the other critical goal of these processes is to obtain "clean" air. This target is ideally met by the exhaustive oxidation of the organic pollutant to CO_2 and water, achieved through several organic oxidation intermediates formed along consecutive and possibly also parallel steps. We therefore performed extensive product analyses under some of the most promising conditions identified in the previous part of the investigation. The combined results of these analyses provided clues to the mechanisms activated by the different corona regimes tested and valuable information to be used in the development of NTP based applications. The reasons why

we focused on EA as model VOC for this study are related to its wide diffusion as a pollutant of indoor air and to its relatively low reactivity in oxidation reactions, a feature which makes it a more challenging target than, for example, hydrocarbons, for testing new air cleaning devices. Thus, the rate constant for the reaction of EA with OH radicals, the oxidant of AOPs (*Advanced Oxidation Processes*), is $1.82 \cdot 10^{-12}$ cm^3 $molecule^{-1}$ s^{-1}, significantly lower than the corresponding values for hexane and of toluene, which are $5.5 \cdot 10^{-12}$ cm^3 $molecule^{-1}$ s^{-1} and $6.1 \cdot 10^{-12}$ cm^3 $molecule^{-1}$ s^{-1}, respectively [13]. Ethyl acetate is found in nature but is also a bulk chemical in the chemical industry, with a yearly market of over 2.5 million tons estimated in 2008 [14]. It is the most common ester found in fruits, produced by different microorganisms, and has a fruity smell which affects significantly the organoleptic characteristics of distillates [15]. Ethyl acetate is one of the best organic solvents and is used in many applications (coatings, varnish removers, inks, glues, perfumes, confections) and processes including the synthesis of pharmaceuticals and organics. Despite its low toxicity, EA is classified as hazardous under the Hazardous Products Regulations (SOR/2015-17), with exposure limits set at 400 ppm (NIOSH REL TWA 400 ppm; OSHA PEL TWA 400 ppm) [16]. Inhalation of EA vapors at and above this level causes irritation of nose, throat, conjunctiva and mucous membrane of the respiratory tract [17-18]. Thus, EA was included in many studies and applications of novel air treatment approaches, including NTP. Rudolph et al. used dielectric barrier discharges (DBD) and studied the kinetics of EA decay as a function of its initial concentration, reaching the conclusion that in humid air the oxidation reaction is initiated by OH radical attack [19]. DBD discharges were also used by Schiavon et al. [20] to treat mixtures of EA and ethanol, which are major components of typical emissions from the printing industry. Maximal CO_2 selectivities of 62-70% and energy yields of 6-11 $g \cdot kW^{-1}$ h^{-1} were obtained in this study [20]. The combined performance of DBD plus catalyst in EA oxidative degradation was also tested in recent works. Using a double DBD reactor Mustafa et al. obtained increased energy efficiency and suppression of unwanted byproducts in the presence of $BaTiO_3$ and HZSM-5 catalysts [21]. Zhu et al. used instead perovskite type catalysts in combination with DBD studying the effect of Ce doping of the catalyst

on the process efficiency. The highest removal efficiency (100%) and COx selectivity (91.8%) were achieved in the plasma-catalytic oxidation of ethyl acetate (initial concentration 100 ppm) over the $La_{0.9}Ce_{0.1}CoO_{3+\delta}$ catalyst at a SED of 558 $J \cdot L^{-1}$ [22]. Wu et al. investigated the effect of novel nanofiber catalysts, nano-V_5Ti and nano TiO_2, and found a significant improvement in efficiency with respect to plasma alone: with the same energy input (580 $J \cdot L^{-1}$) the removal efficiency increased from 50 to 95% [23].

Experimental

Chemicals. 'Air' used in the experiments was a syntethic mixture (80% nitrogen – 20% oxygen) from Air Liquide with specified impurities of H_2O (< 3 ppm) and of C_nH_m (< 0.5 ppm) ('synthetic air'). Ethyl acetate (>99.5% purity) was purchased from Sigma Aldrich and used as received. Ultrapure grade water (milliQ water) was obtained by filtration of deionized water with a Millipore system.

Corona reactor, gas line and experimental procedures. The flow-through corona reactor has a wire cylinder configuration. The cylinder (stainless steel, 38.5 mm i.d. x 600 mm) is electrically grounded and has a small window (10 x 1 cm) cut through its wall for visual inspection of the plasma. The active electrode is a stainless steel wire electrode (1 mm o.d.) fixed along the cylinder axis. The whole assembly is inserted into a pyrex cylinder of slightly wider diameter and made leak-free by means of Teflon caps at both ends. A photograph is show in figure 1.

The reactor was energized by dc or pulsed high-voltage power. The dc power supply ranges were: input voltage 0 – 220 V, output voltage -25 – +25 kV, output current 0 – 5 mA. For pulsed corona discharges a pulsed high voltage was used with dc bias, based on a spark gap switch with air blowing: dc bias 10 – 12 kV, peak voltage 18 kV with dc bias, peak current up to 100 A, frequency 30-200 Hz, rise-time of pulses less than 50 ns. Details are available in previous publications [24, 25].

Figure 1. NTP reactor.

The gas mixture of desired composition in EA (C_0, inlet concentration in ppm) was prepared by bubbling 'synthetic air' through a sample of liquid EA and by diluting the outcoming flow with synthetic air to the desired concentration and flow. After each experiment the reactor was "cleaned" by flowing pure air for several minutes prior to switching to the air/VOC mixture for the next experiment. Before each experiment, the desired initial EA concentration, C_0 was set and verified by GC analysis. The gas flow line is equipped with a loop for humidification and with a probe to measure the humidity. The treated gas is sampled at the reactor outlet for off-line (GC/MS-HP 5973 and GC/FID-Varian 3600) and on-line (FT-IR-Nicolet 5700 spectrophotometer, 10 cm long gas cell and NaCl windows) chemical analyses. Quantification of CO and CO_2 was performed as described previously [24].

All experiments were run at a constant gas flow while changing the applied voltage (dc) or the pulse frequency (+pulsed) and thus the SIE, the Specific Input Energy (kJ/L). The efficiency of the process was then measured by measuring residual EA as a function of SIE, which was determined as described previously for dc [24] and pulsed [25] corona, respectively. Each experiment was carried out at least twice, the repeatability of the results being within 10%.

Current/voltage characteristics of dc corona were monitored both in the presence and in the absence of EA. For each applied voltage the mean current intensity was measured with a multimeter after a stabilization time of 5 minutes.

Analysis of ions. Ion analysis was performed as described previously with an Atmospheric Pressure Chemical Ionization - mass spectrometer (APCI-TRIO 1000 II by Fisons Instruments, Manchester, U.K.) [26-28].

Results and Discussion

Process efficiency

The efficiency of ethyl acetate removal in air by means of NTP treatment was evaluated under different experimental conditions by measuring the residual fraction of the pollutant, C/C_0, as a function of SIE, the *Specific Input Energy*, i.e. the energy applied per unit volume (expressed in kJ/L). Typical decay profiles observed in some representative experiments are shown in figure 2 in which the performance of different energization modes applied within the same corona discharge reactor can be compared and appreciated. The conditions set for this comparison were as follows: ethyl acetate 500 ppm in dry air at a flow of 500 mL/min. The results shown in figure 2 indicate that the process efficiency increases significantly in the order dc+ < dc- < pulsed+, and that for each experiment the data fit approximately a first order exponential decay as a function of SIE. The data were thus fitted using eq. 1

$$C/C_0 = e^{-k_E \cdot SIE} \qquad (1)$$

where C_0 and C are, respectively, the pollutant initial concentration and the residual concentration reached by application of a given SIE, and k_E is the energy constant, one of the parameters used to characterize and compare the energy efficiency of NTP processes [4].
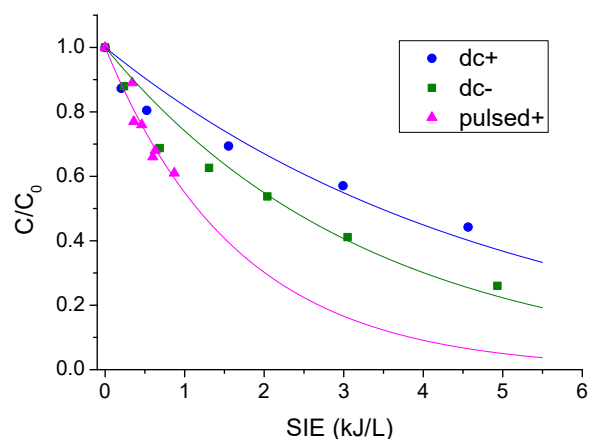
Figure 2. Degradation of ethyl acetate, at 500 ppm initial concentration, in corona reactor powered by pulsed+, dc- and dc+ high voltage. In all experiments the flow rate was 500 mL/min, corresponding to a residence time of 84 s.

Specifically, under the conditions indicated above, k_E values of 0.20, 0.32 and 0.60 kJ/L were determined for dc+, dc- and pulsed+, respectively. These findings are consistent with results obtained earlier with the same reactor in processing different VOCs [24, 25, 29-31], confirming that the energization mode used to generate corona discharges has major effects on the process efficiency.

The effect of humidity was studied next, comparing the decay of ethyl acetate in dry air and in air with a controlled humidity grade of 40% RH, used here as a representative condition for ambient air. The data shown in figure 3(a-c), obtained in experiments run with pulsed+, dc- and dc+, respectively, exemplify the general behavior observed in these systems and highlight the different effects brought about by humidity on the oxidation efficiency in different corona regimes. Notably, the decay of ethyl acetate is more efficient in humid than in dry air for pulsed+ and dc-, whereas there appears to be no effect or, if any, a reduction of efficiency in the experiments with dc+. This behavior, observed previously with other VOCs [24-26, 29-31], is clearly evident also in the experiments, described below, run with different initial concentrations of ethyl acetate.
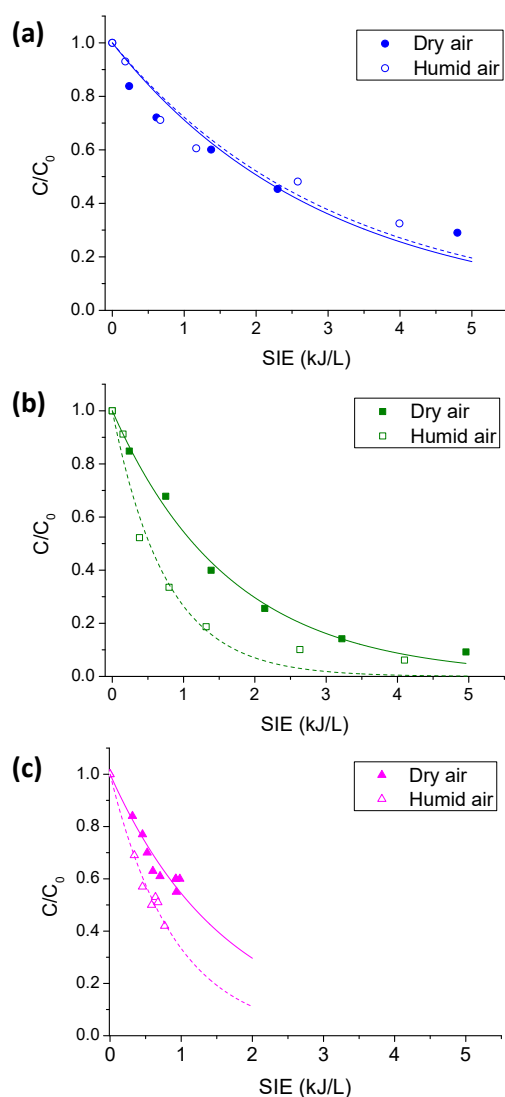
Figure 3. Effect of humidity on the degradation of ethyl acetate, at 250 ppm initial concentration, in corona reactor powered by a) dc+, b) dc- and c) pulsed+. Closed symbols refer to data obtained in dry air, open symbols in air with 40% RH.

In the case of pulsed+, due to circuit limitations, we could not provide SIE > 1 kJ/L. While this energy value was sufficient to decompose almost completely alkanes [25] and toluene [29], it was not for ethyl acetate, notoriously a more recalcitrant VOC in oxidation reactions.

Finally, we investigated the effects on the process efficiency due to changing the initial concentration of ethyl acetate (C_0). The results obtained in experiments with C_0 equal to 250, 500, 750 and 1000

ppm, with dc+ and dc- both in dry and in humid air are collected in Table 1, which reports data of k_E as well as of EY, the *energy yield*, another widely used parameter to assess the process energy efficiency. EY is defined by equation 2 [4]

$$EY \left(\frac{g}{kWh}\right) = 0.15 \cdot \frac{\Delta C \cdot MM}{SIE} \qquad (2)$$

where ΔC (in ppm) is ($C_0 - C$), i.e. the VOC concentration reduction achieved by a given SIE (in J/L), and MM (in g/mol) is the VOC molecular mass. It follows clearly that EY depends directly on the extent of conversion achieved but inversely on the energy required to attain it. Two sets of EY data are reported in Table 1, EY_{50} and EY_{95}, corresponding, respectively, to 50% and 95% conversion. They were calculated using eq. 2 and the k_E data reported in Table 1.

Table 1. Efficiency of ethyl acetate degradation at different initial concentrations in dry and humid air in corona reactor powered by dc- and dc+.

| C_0, ppm	k_E (L/kJ)				EY_{50} (g/kWh)				EY_{95} (g/kWh)			
	dc-		dc+		dc-		dc+		dc-		dc+	
	dry	humid	dry	humid	dry	humid	dry	humid	dry	humid	dry	humid
250	0.61	1.3	0.34	0.33	1.4	3.1	0.81	0.79	0.64	1.4	0.36	0.34
500	0.32	0.75	0.20	0.23	1.5	3.6	0.95	1.1	0.67	1.6	0.42	0.48
750	0.21	0.69	0.21	0.14	1.5	4.9	1.5	1.0	0.66	2.2	0.66	0.44
1000	0.22	0.44	0.11	0.09	2.1	4.2	1.0	0.86	0.46	1.8	0.46	0.38

It is seen that for any of the experienced conditions it always holds that $EY_{95} < EY_{50}$. Considering that both numerator and denominator increase in going from EY_{50} to EY_{95} it follows that the higher

energy required to achieve 95% exceeds in value the corresponding reduction in concentration. This is consistent with the exponential decay of C with SIE and basically means that relatively more and more energy is necessary to degrade a given amount of pollutant as the pollutant concentration becomes lower and lower. It is also seen that the best energy yields are obtained in experiments with dc- in humid air.

Our values of EY_{95} with dc- in humid air are not significantly different from results obtained with other discharges and set ups found in the literature. Mustafa et al. using a cylindrical DBD reactor obtained a EY_{95} of about 0.5 and 1.3 g/kWh for the decomposition of 100 ppm ethyl acetate without and with HZSM-5 as catalyst, respectively [21]. Tu et al., employing a coaxial DBD reactor, achieved EY_{95} values of about 2.6 g/kWh for 100 ppm of ethyl acetate in the presence of $La_{0.9}Ce_{0.1}CoO_{3+\delta}$ perovskite catalyst [22] and 2.2 g/kWh with a novel V_2O_5/TiO_2 nanofiber catalyst [23]. With plasma alone they obtained a EY_{50} of 1.1 g/kWh for the same ethyl acetate initial concentration. A significant higher value of EY_{95}, 11 g/kWh, was obtained by Schiavon et al. with a DBD reactor but under conditions which cannot be directly compared with ours since 780 ppm of ethyl acetate were treated in mixture with 600 ppm of ethanol [20].

Products of corona discharges in air containing ethyl acetate

Volatile products were investigated by means of FT-IR and GC-MS analyses of the gas mixture at the reactor outlet. These products include ozone and NOx, which are also formed in the absence of ethyl acetate, as well as carbon-containing species produced in the advanced oxidation of ethyl acetate, notably CO_2, CO and possible organic oxidation intermediates. FT-IR spectra provide a comprehensive picture of the gas components as shown in the examples reported in figure 4.
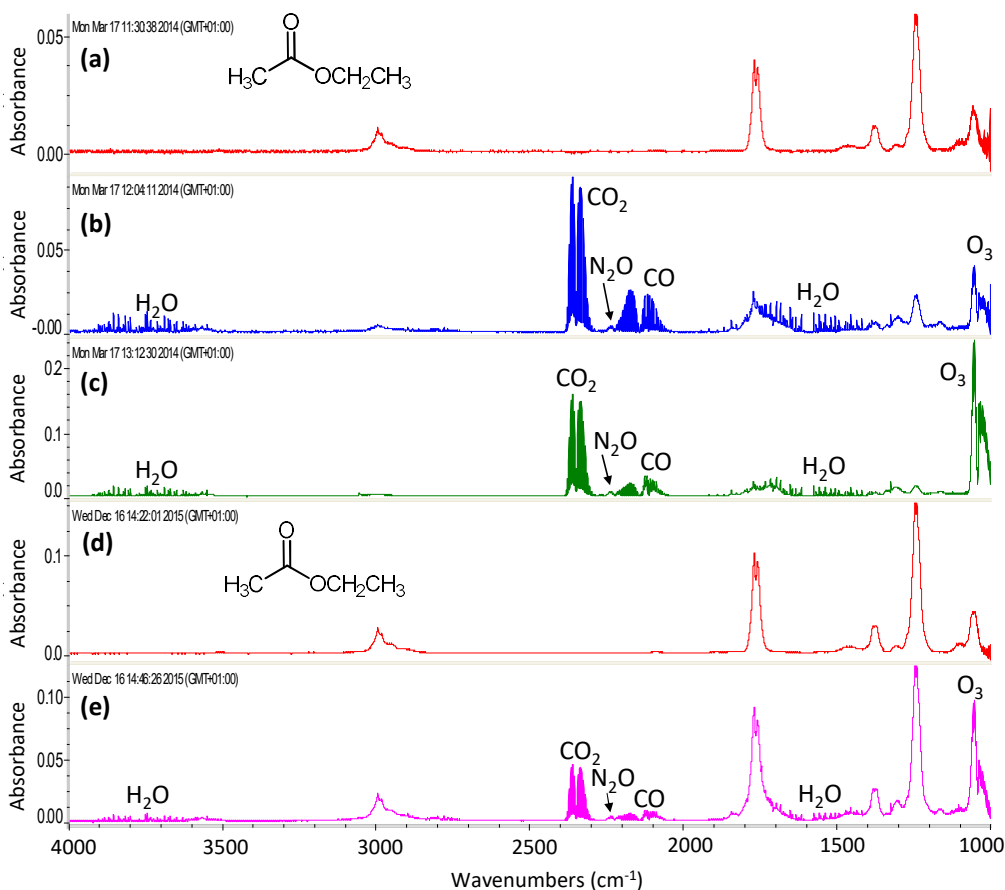
Figure 4. FT-IR spectra of the gas at the reactor outlet. a) EA (250 ppm) in dry air, discharge off; b) EA (C_0 = 250 ppm) in dry air, discharge on, dc+, 21.5 kV (4.6 kJ/L); c) EA (C_0 = 250 ppm) in dry air, discharge on, dc-, 21.5 kV (4.9 kJ/L); d) EA (C_0 = 750 ppm) in dry air, discharge off; e) EA (C_0 = 750 ppm) in dry air, discharge on pulsed+, 18 kV, 200 Hz (0.87 kJ/L).

Panel (a) in figure 4 reports the spectrum of the gas mixture, dry air containing 250 ppm ethyl acetate, at the reactor outlet prior to NTP-processing (discharge was off). This spectrum contains only the characteristic absorption bands of ethyl acetate and serves as reference for the analysis of those shown in panels (b) and (c), which were recorded with the discharge on, dc+ and dc-, respectively. Similarly, the spectrum of panel (d), dry air containing 750 ppm ethyl acetate and discharge off, serves as reference for the spectrum in panel (e), which was recorded with pulsed+ discharge on. Apart from differences in the relative intensities of the various signals, which depend on the type of energization,

11

on the SIE applied and on the EA initial concentration, the three spectra of corona processed gas display the same absorption bands (panels (b), (c) and (e)). Specifically, they all reveal the presence of unreacted residual EA and the characteristic absorptions of CO_2, CO and O_3. In addition, H_2O is also present in the treated gas, clearly formed in the oxidation process since its contribution in the spectrum with the discharge off is barely visible. Exhaustive oxidation of organic compounds indeed produces CO_2 and H_2O. Although the presence of organic oxidation intermediates of EA cannot be excluded, FT-IR analysis lacks the sensitivity and specificity required to detect and identify minor components in the gas mixture. These were thus investigated by means of GC-MS analysis, which allowed us to detect, besides residual EA, a few very minor components, two of which were identified as acetic acid and acetaldehyde, based on their mass spectra and comparison with standards (figure 5).
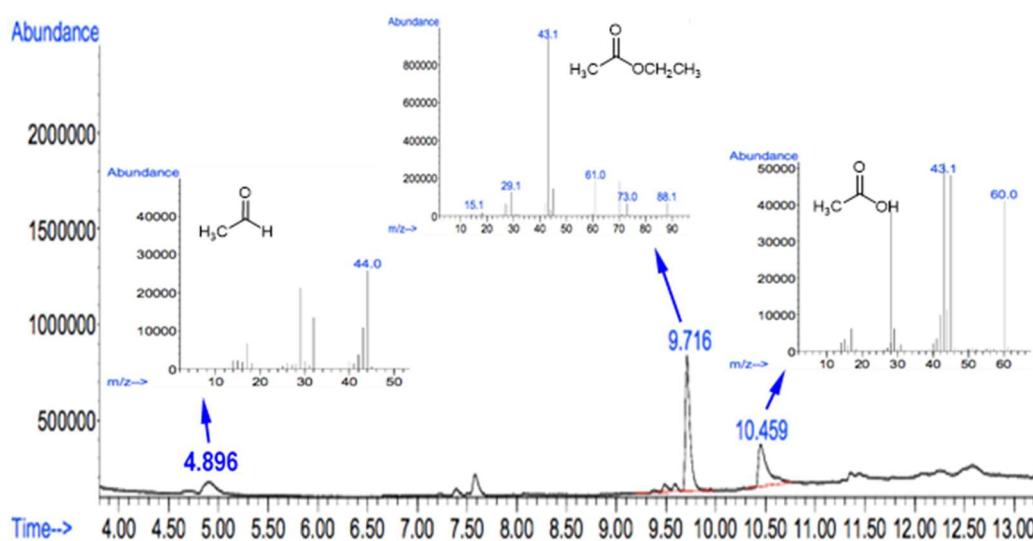
Figure 5. TIC (Total Ion Chromatogram) of gas at the reactor outlet in dc- processing of ethylacetate ($C_0 = 250$ ppm) in dry air. Mass spectra and structural assignments of major peaks are shown in the insets.
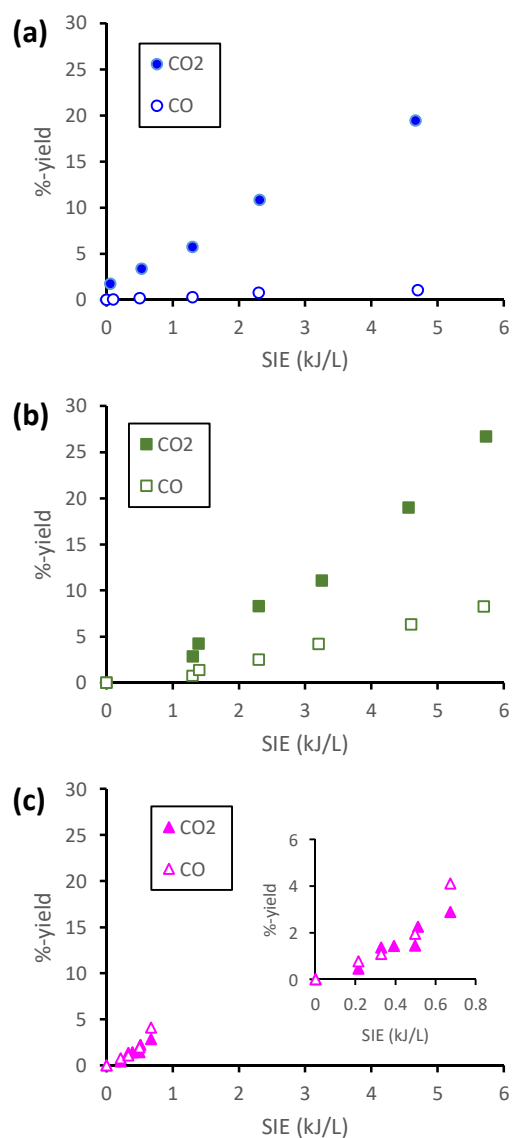
Figure 6. Production of CO and CO_2, expressed as %-yield, in NTP processing of EA in dry air. a) dc+ (EA initial concentration was 250 ppm); b) dc- (EA initial concentration was 250 ppm); c) pulsed+ (EA initial concentration was 750 ppm).

FT-IR spectra were instead useful to quantify the major products of EA NTP processing, notably CO and CO_2. The results of these analyses are summarized in figure 6, with panels (a), (b) and (c) reporting data for dc+, dc- and pulsed+ experiments, respectively. The plots show the %-yields of CO and CO_2 achieved as a function of applied SIE. They were determined according to equations 3 and 4

%-yield CO = 100 · (C_{CO}/4·C_0) $\qquad$ (3)

%-yield CO_2 = 100 · (C_{CO2}/4·C_0) $\qquad$ (4)

where C_0 is the concentration of ethyl acetate before the treatment and C_{CO} and C_{CO2} are those of CO and CO_2 produced.

Mechanisms

The dependence of k_E on C_0, the initial concentration of ethyl acetate, can be used to obtain mechanistic insight into the NTP-induced oxidation reactions. Adapting the procedure originally proposed by Slater and Douglas Hamilton, based on a kinetic model including competition by the reaction intermediates [32], the data reported in Table 1 were used to build plots of k_E *vs* 1/C_0 (figure 7). It is seen that, in good approximation, the data from each set of experiments (dc+ in dry and in humid air; dc- in dry and in humid air) correlate linearly as predicted by the model. According to the model, the slopes of the lines are the efficiency of formation of the reactive species involved in the first step of the VOC oxidation reaction. Their values, in μmol/kJ, are summarized in Table 2.
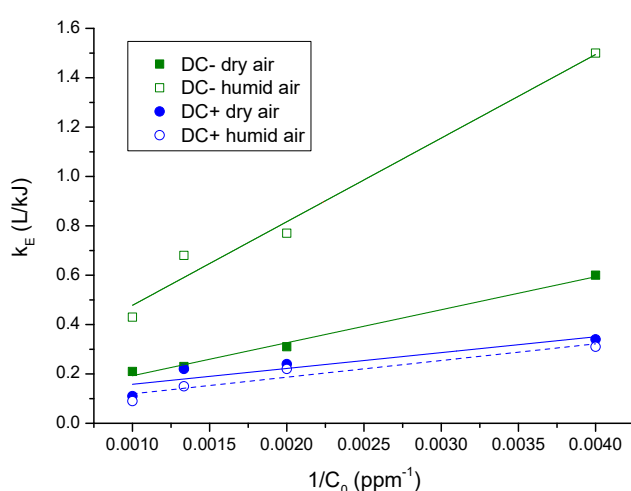
**Figure 7.** Dependence of k_E on EA initial concentration (C_0) in NTP induced oxidation processes in dry and humid (40% RH) air with dc- and dc+.

Table 2. Efficiency and suggested identity of production, in μmol/kJ, of plasma generated reactive species involved in EA first oxidation step under different experimental conditions.[a]

Corona discharge	Gas	Efficiency of production of reactive species [a] (μmol/kJ)	Suggested identity of major reactive species [b]
dc-	dry air	5.4	O atoms, excited nitrogen species
dc-	humid air	14	OH radical
dc+	dry air	2.6	ions ($N_2^+\cdot$, $O_2^+\cdot$, $H_2O^+\cdot$, H_3O^+)
dc+	humid air	2.7	ions ($N_2^+\cdot$, $O_2^+\cdot$, $H_2O^+\cdot$, H_3O^+)

[a]Obtained as the slope of the k_E vs $1/C_0$ linear plots shown in figure 7. For the ppm to μmol/L conversion we assumed that the gas was at standard conditions (298 K and 1 atm). [b]See text for details.

This type of analysis shows first of all that the efficiency of formation of the reactive species in dc-corona is much higher in humid than in dry air. This finding supports the proposal that the reactive species in dc- induced oxidation of EA is the hydroxyl radical, which is formed by reaction of atomic oxygen with water (eq. 5).

$$O(^1D) + H_2O \rightarrow 2\,HO\cdot \qquad (5)$$
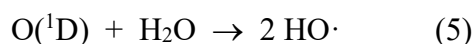
Evidence for the efficient formation of OH radicals by dc- in humid air was obtained in earlier work with the same reactor used in this study [26], by monitoring the well known reaction of CO with OH radicals to give CO_2 [33].

The oxidation of EA in air initiated by the attack of the hydroxyl radical has been thoroughly investigated [34-36]. Both kinetic parameters and products were determined and a mechanism was proposed. A room temperature rate constant of $(1.82 \pm 0.36) \cdot 10^{-12}$ cm^3 $molecule^{-1}$ s^{-1} has been reported [13] for the reaction, which proceeds via H-abstraction involving preferentially the

secondary carbon of the alcohol mojety of the ester [35-36] to form water and a very reactive carbon radical as shown in Scheme 1. In three fast steps this intermediate is converted into acetic acid, a stable species which we were able to detect by GC-MS analysis of the treated gas sampled at the reactor outlet (figure 5). Note that the reaction involves NO which is present in air non-thermal plasma, as well as in our natural atmosphere, and that oxidation of the organic pollutant is coupled with oxidation of NO to NO_2 as indicated in Scheme 1 [13, 36].
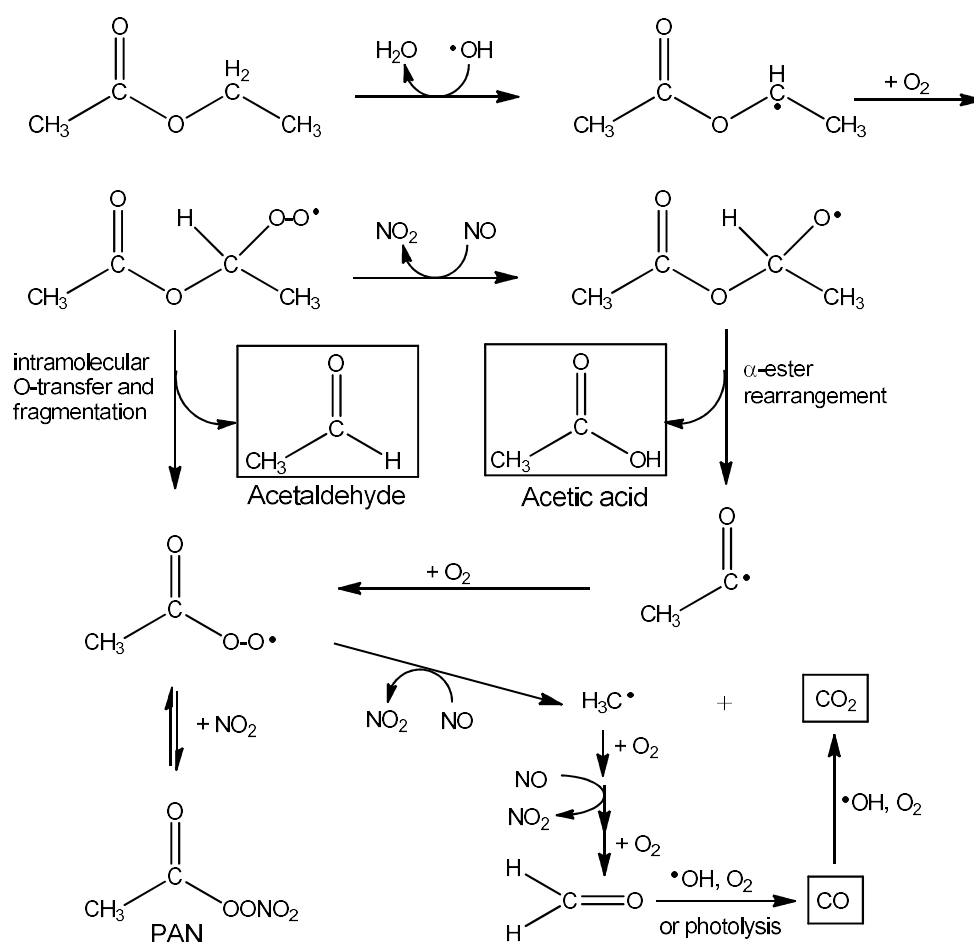
Scheme 1. Reaction pathways for EA oxidation initiated by OH radical. The species enclosed in boxes were detected experimentally.

In addition to acetic acid, we also detected acetaldehyde (figure 5) which can form via intramolecular O-transfer and fragmentation of the peroxoradical intermediate. The other product of this reaction, the acyl peroxo radical $CH_3C(O)OO\cdot$, oxidizes another molecule of NO to NO_2 and fragments to form CO_2 and a CH_3 radical, which in turn is oxidized to CO_2 via the intermediacy of formaldehyde, as shown in Scheme 1. Another possible source for CO, not shown in the scheme, is the photolysis of acetaldehyde [37].

As for the mechanism of EA oxidation with dc- in dry air, it seems reasonable to consider possible reactions with atomic oxygen species and with excited nitrogen species. The second order rate constant for the reaction of ground state oxygen, $O(^3P)$, with EA to form $\cdot OH$ plus other products, is reported to be $5.59 \cdot 10^{-15}$ cm^3 $molecule^{-1}$ s^{-1} at 300 K [38], while we could not find kinetic data in the literature for the reaction of EA with excited oxygen species, notably with $O(^1D)$. However, based on extensive literature compilations regarding several other compounds, the rate constant for the reaction of EA with $O(^1D)$ is expected to be 6-8 orders of magnitude higher than that with $O(^3P)$ [39]. Of course the reaction rate depends not only on the rate constant but also on the reactive species concentration. In previous studies [30, 40] with the same reactor used here, we did detect, by optical emission spectroscopy, excited atomic oxygen in air plasma produced by dc- corona. However, we did not perform quantitative determinations on this species. Finally, excited nitrogen species should be considered. Thus, according to Rudolph et al. [19], excited nitrogen species are involved in the reaction of EA in dry air induced by DBD discharges.

In striking contrast with dc- corona, the presence of humidity in water does not significantly affect the efficiency of EA degradation with dc+ corona (see data in Tables 1 and 2). And this in spite of the fact that in the above mentioned study on the oxidation of CO by OH radicals [26] we found that in humid air OH radicals are produced also by dc+ corona. Thus, it appears that, in contrast with what found for dc- corona, hydroxy radicals are not the major reactive species in EA oxidation with dc+ corona. This conclusion is consistent with earlier reports on dc+ induced advanced oxidation of

aliphatic and aromatic hydrocarbons [24, 26, 29] and of CH_2Br_2 in air [30, 31], tested under similar conditions as used in this work.

One possible alternative considers ion-molecule reactions. The current/voltage profiles reported in figure 8 show that in dc+ the current measured in the presence of 500 ppm of EA was significantly lower than in pure air (panel (a). The effect appears to be further increased in humid air. In contrast, virtually no effect is observed in the case of dc- (figure 8, panel (b), the three curves (pure dry air, dry air plus 500 ppm EA and humid air plus 500 ppm EA) being almost overlapped. Information on the ions present in these systems is necessary to analyze and rationalize these findings since the conduction of charge in air at atmospheric pressure is due to ion transport. The mass spectra of pure air and of air containing EA subjected to dc+ and dc- corona discharges are shown in figure 8. In the case of dc- there appears to be no significant effect due to the presence of EA in the mass spectrum which is dominated by signals due to $O_2^{-\bullet}$, $O_3^{-\bullet}$ and their hydrates (figures 8(e) and 8(f)). Correspondingly, no effect is seen in the discharge current (figure 8(b)). In contrast, in the case of dc+ the presence of EA, albeit in very low concentration, modifies completely the mass spectrum. Thus, while the major ions detected in pure air are H_3O^+ and $H_3O^+(H_2O)$ (figure 8(c)) in the presence of EA they are protonated EA, EA·H^+, and a fragment with m/z 61, which is identified as protonated acetic acid (figure 8(d)). Considering that different ions have different mobilities [41], it is not surprising that the different mass spectra observed in pure air and in air doped with 500 ppm EA (figures 8(c) and (d)) are matched by different current/voltage profiles (figure 8(a)). Thus, both types of measurements (discharge current and mass spectra) provide a self-consistent picture which reflects the fact that the equilibrium ion populations generated by dc+ in air and in air containing EA are quite different.
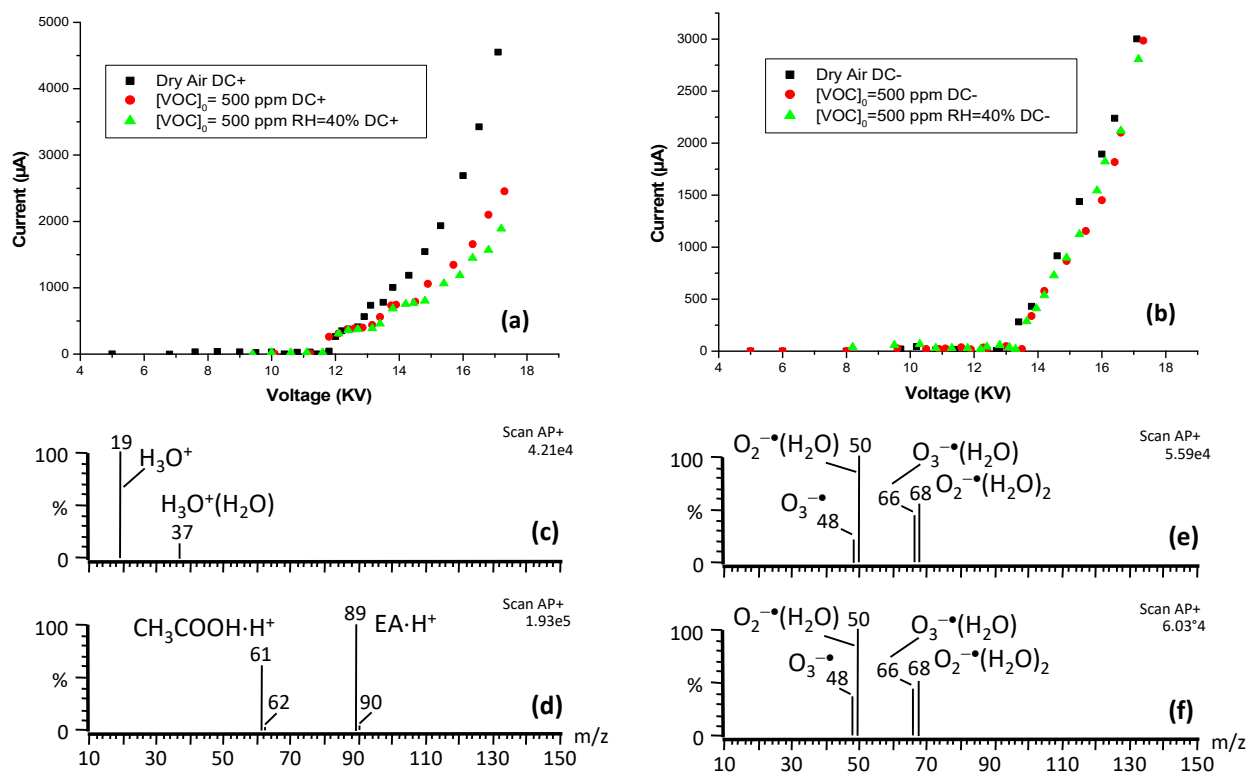
Figure 8. Current/voltage profiles for a) dc+ and b) dc- corona in pure dry air, dry air containing EA (500 ppm) and humid air (40% RH) containing EA (500 ppm). Atmospheric pressure mass spectra in positive polarity of c) dry air and d) dry air containing EA under dc+ corona discharges and in negative polarity of e) dry air and f) dry air containing EA under dc- corona discharges.

The suppression of the characteristic ions of pure air in dc+ plasma observed in the presence of EA are rationalized considering that the proton affinity of EA (835.7 kJ mol^{-1}) is much higher than that of water (691 kJ mol^{-1}) [42] and that exothermic proton transfer reactions are very fast at atmospheric pressure. The ion chemistry of protonated EA formed by dc+ in air at atmospheric pressure is better illustrated in figure 9, which reports relative intensities of the major ions detected as a function of the fragmentation potential set up on the instrument (figure 9). The ion chemistry of several esters, including ethyl acetate, in air at ambient pressure was investigated and reported in detail in a previous publication [28].

19
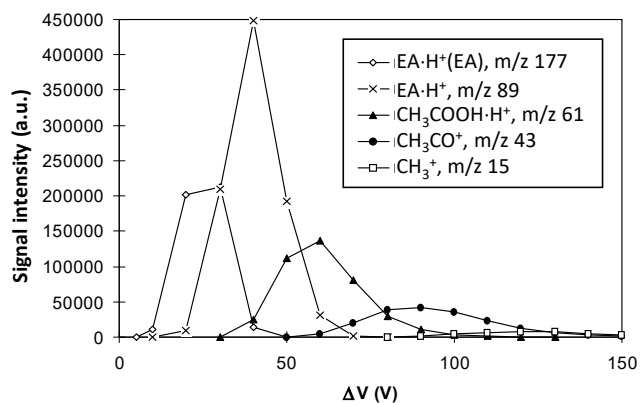
Figure 9. Plot of the intensity of the signals observed in the positive mass spectra of ethyl acetate in dry air as a function of the instrumental fragmentation potential.

Interestingly, these analyses provide evidence for a possible ionic pathway leading to acetic acid via fragmentation of $EA \cdot H^+$ followed by fast exothermic proton transfer (the proton affinity of acetic acid is 783.7 kJ/mol [42]) as shown in Scheme 2.
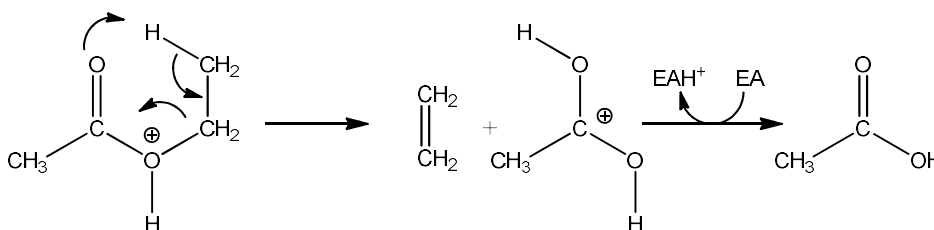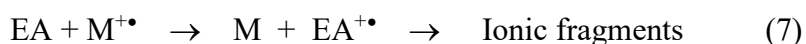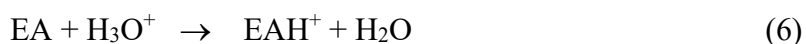

Scheme 2. Ionic route to acetic acid.

Conclusions

The results of this study confirm the capabilities of air non-thermal plasma to induce the degradation of volatile organic pollutants in air at room temperature and ambient pressure even in the case of relatively resistant compounds such as the oxygen-rich organic solvent ethyl acetate. They also show that the strong oxidizing power of such plasmas leads to efficient mineralization of organic carbon, as we found that CO_2 (together with, under some conditions, CO) was the main carbon-containing

product at any value of EA conversion, the major oxidation intermediates, acetic acid and acetaldehyde, being detected only in very small amounts. The results also allow for the direct comparison of the performance of three corona discharges (pulsed+, dc- and dc+) tested on common ground, i.e. within the same reactor and under the same experimental conditions. Consistently with earlier findings reported in the literature, including some from our own laboratory, positive pulsed corona discharges proved superior to dc corona discharges in bringing about the degradation of EA in air. However, quite satisfactory results were also obtained with dc- corona especially in humid air, using a simple, sturdy, stable and easy to operate power supply. Thus, dc- appears to be an interesting asset in view of practical applications which, depending on the volume of air to be treated, could implement a proper number of modules connected in parallel. Another favorable feature of dc- is the beneficial effect of humidity, as is typically found in ambient air, which increases significantly the efficiency of dc- corona processing of EA, in sharp contrast with what found with dc+. The results obtained in this study allow us to advance mechanistic proposals for the initial step of EA oxidation under the different experimental conditions tested. Specifically, as summarized in Table 2, it is suggested that neutral reactive species are involved in the case of dc-, notably the OH radical in humid air and atomic oxygen and/or excited nitrogen species in dry air, respectively. In contrast, ion molecule reactions appear to be primarily involved in case of dc+ corona, as outlined in equations 6 and 7

$$EA + H_3O^+ \quad \rightarrow \quad EAH^+ + H_2O \qquad\qquad (6)$$

$$EA + M^{+\bullet} \quad \rightarrow \quad M \ + \ EA^{+\bullet} \quad \rightarrow \quad \text{Ionic fragments} \qquad (7)$$

where M can be any of N_2, O_2, H_2O. Both proton transfer (6) and charge transfer (7) reactions are highly exothermic and thus expected to proceed virtually at collision rate.

References

1. Schiavon M, Torretta V, Casazza A and Ragazzi M 2017 Non-thermal plasma as an innovative option for the abatement of volatile organic compounds: a Review *Water Air Soil Pollut.* **228** 388

2. Xiao G, Xu W, Wu R, Ni M, Du C, Gao X, Luo Z and Cen K 2014 Non-thermal plasmas for VOCs abatement *Plasma Chem. Plasma Process.* **34** 1033–1065

3. Vandenbroucke A M, Morent R, De Geyter N and Leys C 2011 Non-thermal plasmas for non-catalytic and catalytic VOC abatement *J. Hazard. Mater.* **195** 30–54

4. Kim H H 2004 Nonthermal plasma processing for air-pollution control: a historical review, current issues, and future prospects *Plasma Process. Polym.* **1** 91–110

5. Fridman A 2008 *Plasma chemistry* Cambridge: Cambridge University Press

6. Jiang N, Guo L, Qiu C, Zhang Y, Shang K, Lu N, Li J and Wu Y 2018 Reactive species distribution characteristics and toluene destruction in the three-electrode DBD reactor energized by different pulsed modes *Chem. Eng. J.* **350** 12-19

7. Yao X, Jiang N, Li J, Lu N, Shang K and Wu Y 2019 An improved corona discharge ignited by oxide cathodes with high secondary electron emission for toluene degradation *Chem. Eng. J.* **362** 339-348

8. Jung S, Fang J, Chadha T S and Biswas P Atmospheric pressure plasma corona enhanced by photoionizer for degradation of VOCs 2018 *J. Phys. D: Appl. Phys.* **51** 445206

9. Zhang Z, Jiang Z and Shangguan W Low-temperature catalysis for VOCs removal in technology and application: A state-of-the-art review 2016 *Catalysis Today* **264** 270-278

10. Kim H H, Teramoto Y, Ogata A, Takagi H and Nanba T 2016 Plasma catalysis for environmental treatment and energy applications *Plasma Chem. Plasma Process.* **36**, 45-72

11. Huang Y, Dai S, Feng F, Zhang X, Liu Z and Yan K 2015 A comparison study of toluene removal by two-stage DBD-catalyst systems loading with MnOx, CeMnOx, and CoMnOx *Environ. Sci. Pollut. Res.* **22** 19240-19250

12. Thevenet F, Sivachandiran L, Guaitella O, Barakat C and Rousseau A 2014 Plasma-catalyst coupling for volatile organic compound removal and indoor air treatment: A review *J. Phys. D: Appl. Phys.* **47** 224011

13. Atkinson R 1985 Kinetics and mechanisms of the gas-phase reactions of the hydroxyl radical with organic compounds under atmospheric conditions *Chem. Rev.* **85** 69-201

14. ICIS Chemical Business (ICB), see www.icis.com

15. Dionísio A P, Molina G, Souza de Carvalho D, Dos Santos R, Bicas J L and Pastore G M 2012 Natural flavourings from biotechnology for foods and beverages in *Natural Food Additives, Ingredients and Flavourings* Eds. David Baines, Richard Seal, In Woodhead Publishing Series in Food Science, Technology and Nutrition, Natural Food Additives, Ingredients and Flavourings, Woodhead Publishing, pp. 447-460

16. The National Institute for Occupational Safety and Health (NIOSH) https://www.cdc.gov/niosh/npg/npgd0260.html

17. The MAK‑Collection for Occupational Health and Safety: Annual Thresholds and Classifications for the Workplace 2011 Wiley‑VCH Verlag GmbH & Co. KGaA https://doi.org/10.1002/3527600418.mb14178e0012

18. MSDS Ethyl acetate, MSDS No E2850 [Online], Mallenckrodt Baker, Phillipsburg, NJ, Nov 12, 2001.

19. Rudolph R, Francke K P and Miessner H 2002 Concentration dependence of VOC decomposition by dielectric barrier discharges *Plasma Chem. Plasma Process.* **22** 401-412

20. Schiavon M, Scapinello M, Tosi P, Ragazzi M, Torretta V and Rada E C 2015 Potential of non-thermal plasmas for helping the biodegradation of volatile organic compounds (VOCs) released by waste management plants *J. Clean. Prod.* **104** 211-219

21. Mustafa M F, Fu X, Liu Y, Abbas Y, Wang H and Lu W 2018 Volatile organic compounds (VOCs) removal in non-thermal plasma double dielectric barrier discharge reactor *J. Hazard. Mater.* **347** 317-324

22. Zhu X, Zhang S, Yang Y, Zheng C, Zhou J, Gao X and Tu X 2017 Enhanced performance for plasma-catalytic oxidation of ethyl acetate over $La_{1-x}Ce_xCoO_{3+\delta}$ catalysts *Appl. Catal. B: Environ.* **213** 97-105

23. Wu J, Zhu X, Cai Y, Tu X and Gao X 2019 Coupling nonthermal plasma with V_2O_5/TiO_2 nanofiber catalysts for enhanced oxidation of ethyl acetate *Ind. Eng. Chem. Res.* **58** 2-10

24. Marotta E, Callea A, Rea M and Paradisi C 2007 DC corona electric discharges for air pollution control. Part 1. Efficency and products of hydrocarbon processing. *Environ. Sci. Technol.* **41** 5862-5868

25. Marotta E, Callea A, Ren X, Rea M and Paradisi C 2007 A mechanistic study of pulsed corona processing of hydrocarbons in air at ambient temperature and pressure. *Int. J. Plasma Environ. Sci. Tecnhnol*. **1** 39-45.

26. Marotta E, Callea A, Ren X, Rea M and Paradisi C 2008 DC corona electric discharges for air pollution control. Part 2. Ionic intermediates and mechanisms of hydrocarbon processing *Plasma Process. Polym.* **5** 146-154

27. Marotta E, Scorrano G and Paradisi C 2005 Ionic reactions of chlorinated VOCs in air plasma at atmospheric pressure *Plasma Proc. Polym.* **3** 209-217

28. Marotta E and Paradisi C 2005 Positive ion chemistry of esters of carboxylic acids in air plasma at atmospheric pressure *J. Mass Spectrom.* **40**1583-1589

29. Schiorlin M, Marotta E, Rea M and Paradisi C 2009 A comparison of toluene removal in air at atmospheric conditions by different corona discharges *Environ. Sci. Technol.* **24** 9386-9392

30. Marotta E, Schiorlin M, Rea M and Paradisi C 2010 Products and mechanisms of the oxidation of organic compounds in atmospheric air plasmas *J. Phys. D - Appl. Phys.* **43** 124011

31. Schiorlin M, Marotta E, Dal Molin M and Paradisi C 2013 Oxidation mechanisms of CF_2Br_2 and CH_2Br_2 induced by air nonthermal plasma *Environ. Sci. Technol.* **47** 542-548

32. Slater C and Douglas-Hamilton D H 1981 Electron beam initiated destruction of low concentration of vinyl chloride in carrier gases *J. Appl. Phys.* **9** 5820-5828.

33. IUPAC Task Group on Atmospheric Chemical Kinetic Data Evaluation – Data Sheet HOx_VOC10, http://iupac.pole-ether.fr/htdocs/datasheets/pdf/HOx_VOC10_HO_CO.pdf.

34. Andersen V F, Berhanu T A, Nilsson E J, Jorgensen S, Nielsen O J, Wallington T J and Johnson M S 2011 Atmospheric chemistry of two biodiesel model compounds: methyl propionate and ethyl acetate *J. Phys. Chem.* **115** 8906-8919

35. Picquet-Varrault B, Doussin J- F, Durand-Jolibois R and Carlier, P 2001 FTIR spectroscopic study of the OH-induced oxidation of two linear acetates: Ethyl and n-propyl acetates *Phys. Chem. Chem. Phys.* **3** 2595-2606

36. Tuazon E C, Aschmann S M, Atkinson R and Carter W P L 1998 The reactions of selected acetates with the OH radical in the presence of NO: novel rearrangement of alkoxy radicals of structure RC(O)OCH(O)R *J. Phys. Chem. A* **102** 2316-2321

37. Atkinson R 1994 Gas-phase tropospheric chemistry of organic compounds *J. Phys. Chem. Ref. Data (monograph 2)* 1-216

38. Herron J T 1988 Evaluated chemical kinetic data for the reactions of atomic oxygen O(3P) with saturated organic compounds in the gas phase *J. Phys. Chem. Ref. Data* **17** 967-102

39. *Selectivity in Chemical Reactions* 1988 NATO ASI Series, Edited by Whitehead J C, Springer, Dordrecht

40. Zaniol B, Schiorlin M, Gazza E, Marotta E, Ren X, Puiatti M, Rea M, Sonato P, Paradisi C 2008 An emission spectroscopy study of atmospheric plasmas formed by DC and pulsed corona discharges in hydrocarbon contaminated air *Int. J. Plasma Environ. Sci. Technol.* **2** 65-71

41. Gabelica V and Marklund E 2018 Fundamentals of ion mobility spectrometry *Curr. Op. Chem. Biol.* **42** 51-59

42. Lias S G 2006 Ionization Energy Evaluation. In NIST Chemistry WebBook, NIST Standard Reference Database No. 69, Maillard W G and Linstrom P J Eds., National Institute of Standards and Technology, Gaithersburg MD, http://webbook.nist.gov/chemistry.